Improved photosynthetic capacity and photosystem I oxidation via heterologous metabolism engineering in cyanobacteria

María Santos-Merino[a], Alejandro Torrado[b], Geoffry A. Davis[a], Annika Röttig[b], Thomas S. Bibby[b], David M. Kramer[a,c], and Daniel C. Ducat[a,c,1]

[a]MSU-DOE Plant Research Laboratory, Michigan State University, East Lansing, MI 48824; [b]Ocean and Earth Science, University of Southampton, SO14 3ZH Southampton, United Kingdom; and [c]Department of Biochemistry and Molecular Biology, Michigan State University, East Lansing, MI 48824

Edited by Krishna K. Niyogi, University of California, Berkeley, CA, and approved February 3, 2021 (received for review October 21, 2020)

Cyanobacteria must prevent imbalances between absorbed light energy (source) and the metabolic capacity (sink) to utilize it to protect their photosynthetic apparatus against damage. A number of photoprotective mechanisms assist in dissipating excess absorbed energy, including respiratory terminal oxidases and flavodiiron proteins, but inherently reduce photosynthetic efficiency. Recently, it has been hypothesized that some engineered metabolic pathways may improve photosynthetic performance by correcting source/sink imbalances. In the context of this subject, we explored the interconnectivity between endogenous electron valves, and the activation of one or more heterologous metabolic sinks. We coexpressed two heterologous metabolic pathways that have been previously shown to positively impact photosynthetic activity in cyanobacteria, a sucrose production pathway (consuming ATP and reductant) and a reductant-only consuming cytochrome P450. Sucrose export was associated with improved quantum yield of phtotosystem II (PSII) and enhanced electron transport chain flux, especially at lower illumination levels, while cytochrome P450 activity led to photosynthetic enhancements primarily observed under high light. Moreover, coexpression of these two heterologous sinks showed additive impacts on photosynthesis, indicating that neither sink alone was capable of utilizing the full "overcapacity" of the electron transport chain. We find that heterologous sinks may partially compensate for the loss of photosystem I (PSI) oxidizing mechanisms even under rapid illumination changes, although this compensation is incomplete. Our results provide support for the theory that heterologous metabolism can act as a photosynthetic sink and exhibit some overlapping functionality with photoprotective mechanisms, while potentially conserving energy within useful metabolic products that might otherwise be "lost."

cyanobacteria | photosynthesis | photoprotection | photoproduction | metabolic engineering

Cyanobacteria, equipped with photosynthetic machinery to fix CO_2 into reduced forms, have been increasingly engineered as biotechnological platforms for light-driven production of a wide variety of bioproducts (1). However, although the theoretical maximum efficiency of solar-to-biomass energy conversion in cyanobacteria has been estimated as 8 to 10%, the best sustained efficiencies that have been reported are in the range of 1 to 2% (2). A major loss to photosynthetic efficiency occurs when source energies (absorbed solar radiation) exceed the capacity of sink metabolism (total cellular energy demand), resulting in increased activation of dissipative photoprotection mechanisms (3). Balancing source/sink energies is one strategy for improving photosynthetic efficiency, and this has typically been pursued by dampening the light energy that is absorbed by cyanobacteria (2, 4), though it has been hypothesized more recently that enhancing sink capacity through rewiring downstream metabolism may achieve similar effects (5).

Cyanobacterial alternative electron transport pathways that accept electrons in the electron transport chain (ETC) and catalyze the reduction of O_2 to water to avoid the uncontrolled formation of damaging reactive oxygen species, include flavodiiron proteins (FDPs) and respiratory terminal oxidases (RTOs) (Fig. 1) (6, 7). Electron flux to RTO and FDP pathways still contribute to proton motive force formation; FDP water–water cycle activity is located downstream of proton-pumping complexes of the ETC (8), and cytochrome oxidase (COX) also directly pumps protons to the lumen (9) (Fig. 1). Nonetheless, by effectively short-circuiting the canonical linear flow of electrons through the ETC, the activity of FDPs and RTOs decrease photosynthetic generation of reducing equivalents (e.g., NADPH) and reduce conversion of potential energy into biomolecules. While the mechanisms underlying the regulation of these pathways have not been elucidated, it is clear that electron flux to them can be dynamically altered on short time scales (seconds to minutes) (10). These mechanisms have been found to be important for energy homeostasis, especially in dynamic environments such as fluctuating light intensities, where they may assist in balancing the overreduction of the ETC (11–13). There is evidence that FDPs and RTOs can exhibit prolonged activity even under controlled-light laboratory conditions, potentially consuming a significant portion of electrons originating

Significance

Cyanobacteria have been increasingly explored as a biotechnological platform, although their economic feasibility relies in part on the capacity to maximize their photosynthetic, solar-to-biomass energy conversion efficiency. Here we show that cyanobacterial photosynthetic capacity can be increased by diverting cellular resources toward heterologous, energy-storing metabolic pathways and by reducing electron flow to photoprotective, but energy-dissipating, oxygen reduction reactions. We further show that these heterologous sinks can partially contribute to photosystem I (PSI) oxidation, suggesting an engineering strategy to improve both energy storage capacity and robustness by selective diversion of excess photosynthetic capacity to productive processes.

Author contributions: M.S.-M., T.S.B., D.M.K., and D.C.D. designed research; M.S.-M., A.T., G.A.D., and A.R. performed research; M.S.-M., A.T., G.A.D., and A.R. analyzed data; and M.S.-M. and D.C.D. wrote the paper.

The authors declare no competing interest.

This article is a PNAS Direct Submission.

[1]To whom correspondence may be addressed. Email: ducatdan@msu.edu.

This article contains supporting information online at https://www.pnas.org/lookup/suppl/doi:10.1073/pnas.2021523118/-/DCSupplemental.

Published March 8, 2021.

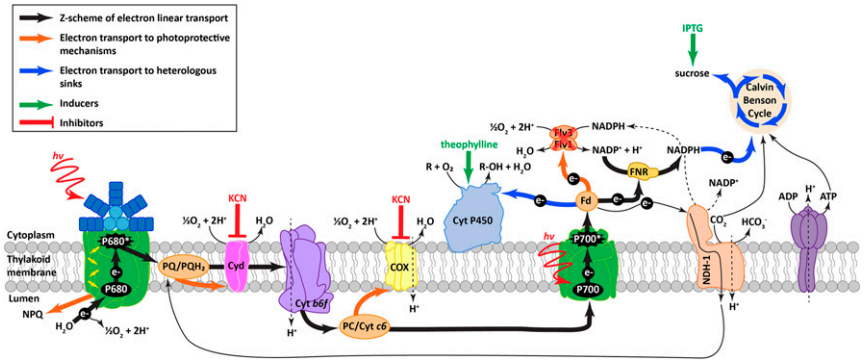

Fig. 1. Overview of ETC, photoprotective mechanisms, and heterologous sinks in *S. elongatus*. When excess energy is absorbed in the light reactions of photosynthesis, it can result in damage to the photosystems and photoinhibition. Energy can be dissipated before charge separation as heat and fluorescence by nonphotochemical quenching (NPQ) mediated by NPQ ascribed to state transitions, a change in the relative antenna size of PSI and PSII. Energy can also be dissipated after charge separation via electron transfer to major electron acceptors, FDPs (Flv3 and Flv1), and to alternative acceptors, RTOs (Cyd and COX) during photoprotection. NADH dehydrogenase-like complex 1 (NDH-1) participates in cyclic electron flux around PSI and CO_2 acquisition.

from water splitting in the photosystem II (PSII) in certain conditions and species (14, 15).

Sink engineering is a recent strategy that is under investigation to improve photosynthetic efficiency in cyanobacteria by improving source/sink energy balance. The expression of a number of distinct heterologous metabolic pathways has been demonstrated to improve photosynthetic properties, such as in strains engineered with carbon sinks [e.g., sucrose (16, 17), 2,3-butanediol (18), isoprene (19), and glycerol (20)], or electron sinks [e.g., cytochrome P450 (21–24)]. One explanation proposed for these observations is that the additional metabolic costs (i.e., ATP and/or NADPH) associated with the expression of the heterologous metabolic pathway utilizes the "overcapacity" of the ETC under sink-limited conditions, increasing the intensity at which photosynthesis becomes saturated or reducing loss of potential energy in the ETC to photoprotective mechanisms. This hypothesis remains to be rigorously tested.

We reasoned that if heterologous metabolic pathways can act to capture excess energy within sink-limited photosynthetic systems, such engineered pathways might exhibit competition with one another or endogenous photoprotective pathways. Indeed, if heterologous metabolism competes substantially with FDPs and RTOs, they might exhibit latent photoprotective qualities themselves. To explore these possibilities, we examined the interplay between two different heterologous sinks (sucrose export and cytochrome P450) in *Synechococcus elongatus* PCC 7942, and compared their competition with native photoprotective sinks (FDPs and RTOs). Surprisingly, we found that a single heterologous sink alone does not appear to utilize the full ETC overcapacity. Furthermore, our data suggest that under specific conditions, these engineered sinks may be used to redirect energy away from less energetically efficient pathways and increase energy stored in more useful metabolic products.

Results

Expression of a Single Heterologous Sink Leads to Distinct Photosynthetic Enhancements. We validated the effect of expressing a carbon sink (sucrose production) (16, 17) or an electron sink (cytochrome P450) (21, 22) separately in *S. elongatus* (Fig. 1). In the case of the previously reported inducible

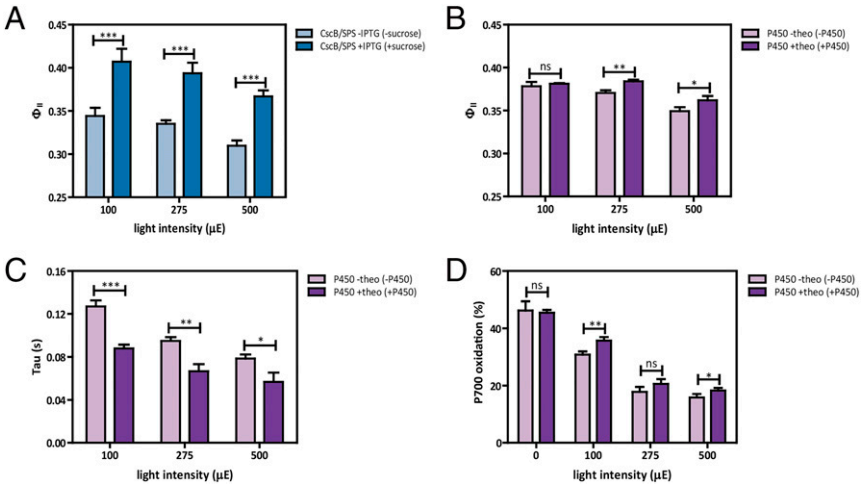

Fig. 2. Engagement of heterologous sinks enhances indicators of photosynthesis. (*A*) Φ_{II} values measured at three different light intensities 24 h after the induction of sucrose export. (*B*) Φ_{II} values measured at three different light intensities 24 h after the induction of cytochrome P450 activity. (*C*) $P700^+$ τ values (in seconds) measured at three different light intensities 24 h after the induction of cytochrome P450 activity. (*D*) P700 oxidation levels, expressed as percentage of a completely oxidized PSI pool, measured at four different light intensities 24 h after the induction of cytochrome P450 activity. Averages of ≥3 independent biological replicates are shown with SD reported with error bars. Significance was calculated by unpaired Student's *t* test relative to uninduced strain as control. $*P < 0.05$, $**P < 0.01$, $***P < 0.001$; ns, not significant.

sucrose export system (16), genes for sucrose phosphate synthase (SPS) and sucrose permease (CscB) are controlled by isfopropyl-β-D-thiogalactopyranoside (IPTG) and facilitate the accumulation of cytosolic sucrose and its export from the cell, respectively. A second heterologous electron sink consisting of the cytochrome P450 protein, CYP1A1, was originally characterized in *Synechococcus* sp. PCC 7002 (21, 22). CYP1A1 is able to utilize reductant generated from the photosynthetic ETC to catalyze a monooxygenase reaction, and has been successfully used to detoxify the herbicide atrazine, a widespread environmental pollutant (25, 26). When expressed in *Synechococcus* sp. PCC 7002 (22), CYP1A1 expression increased atrazine resistance, improved photosynthetic flux at higher light intensities, and potentially catalyzed monooxygenase reactions with other cytosolic substrates. We constructed an expression cassette carrying the *cyp1a1* gene controlled by a *conII* promoter with a theophylline riboswitch regulator (27). These expression cassettes were independently evaluated for photosynthetic impacts after integrating them into the genome of *S. elongatus*.

We first evaluated the effect of heterologous sinks on the activity of PSII, beginning with the quantum yield of PSII (Φ_{II}), a parameter that estimates the fraction of light absorbed by PSII-associated antenna complexes used for photochemistry at a given actinic light intensity (28, 29). As expected (16), we observed strong induction of secreted sucrose following induction of CscB and SPS (*SI Appendix*, Fig. S1*A*), and this was associated with an increase of Φ_{II} values upon sucrose export (Fig. 2*A*). The expression of cytochrome P450 (*SI Appendix*, Fig. S1*B*) led to a significant increase in cytochrome P450 activity, as measured by the fluorometric ethoxyresorufin-O-deethylase (EROD) assay (*SI Appendix*, Fig. S1*C*), and an increase in the quantum efficiency of PSII (Fig. 2*B*) that was modest at illumination near the growth intensity (100-μmol photons m^{-2} s^{-1}), and becomes significant at higher light intensities (≥275-μmol photons m^{-2} s^{-1}). These results are generally in agreement with prior observations reported for CYP1A1 expression in *Synecococcus* sp. PCC 7002 (22). It should be noted that slight changes in basal levels of Φ_{II} were observed in different genetic backgrounds (*SI Appendix*, Fig. S2), which is not unexpected when comparing between different genotypes (see ref. 30 for detailed explanation). The effect of either sink on photochemical quenching (q_P), an estimate of PSII redox state (31), was more modest and was only statistically significant at selected actinic illuminations for the sucrose sink (*SI Appendix*, Fig. S3*A*) and cytochrome P450 sink (*SI Appendix*, Fig. S3*B*).

Next, we evaluated the effect of the expressing heterologous sinks on electron transport to photosystem I (PSI) using $P700^+$ rereduction kinetics. First, we measured the time constant of dark P700 decay (reduction) in PSI using dark-interval relaxation kinetics (DIRK) (32), an indicator of the steady-state electron flux to PSI [e.g., from cytochrome b_6f (33)]. The $P700^+$ rereduction kinetics were fitted to single exponential decays, and the resulting rate constants (τ) are indicative of electron transfer to the donor side of PSI. Based on the half-time of the decay kinetics, an increased rate of $P700^+$ rereduction during a dark pulse was observed following cytochrome P450 expression (Fig. 2*C*). Moreover, an increase in P700 oxidation under prolonged exposure to constant actinic light was also observed (Fig. 2*D*). One possible explanation for this observation is that cytochrome P450 activity may consume excess reductant from the acceptor side of PSI. Because there is a linear relationship of P700 oxidation to alleviation of PSI photoinhibition (34), this may be indicative of less PSI photodamage when cytochrome P450 is active. This result is similar to strains of *Synechocystis* sp. PCC 6803 engineered for ethylene production, where a decrease in $P700^+$ rereduction half-time was also indicative of increased electron flux through the ETC relative to wild-type background (35). In contrast, no effects on τ values (*SI Appendix*, Fig. S3*C*) or P700 oxidation levels (*SI Appendix*, Fig. S3*D*) were observed following sucrose export.

Coexpression of More than One Heterologous Sink Has Additive Photosynthetic Effects. To evaluate the interplay between multiple heterologous sinks, we constructed strains with independent control of expression of both the sucrose export mechanism (IPTG induced) and CYP1A1 (theophylline induced). Activation of either CYP1A1 or sucrose export in this genetic background led to changes in photosynthetic parameters that matched trends shown previously (i.e., in Φ_{II}, τ, and P700 oxidation) (Fig. 2 *B–D*, respectively), while simultaneous activation of both sinks often led to additive effects. For example, higher quantum efficiencies of PSII were observed in strains with both sucrose and cytochrome P450 sinks activated, and this effect was most pronounced at higher light intensities (≥275-μmol photons m^{-2} s^{-1}) (Fig. 3*A*). The differences in calculated Φ_{II} values were mainly due to an increase of the maximum fluorescence level in the light (F'_M) rather than changes in the steady-state fluorescence level (F_s) (*SI Appendix*, Fig. S4). Furthermore, declining in PSII yields at higher light intensities is an expected outcome of saturating photosynthetic processes; this effect was diminished when both sucrose and cytochrome P450 sinks were activated (Fig. 3*A*). Similarly, P700 was maintained at a higher oxidation state with both sinks activated, especially at higher illumination (Fig. 3*B*). In contrast, the time constant of $P700^+$ rereduction was slightly decreased under conditions when CYP1A1 was expressed, and sucrose sink activation had little effect on this parameter (Fig. 3*C*). Moreover, estimates of the relative electron transport rate (rETR) increased with either CYP1A1 or sucrose export, but were most improved when both sinks were active (Fig. 3*D*). Estimates of PSII (ETR_{II}) activity relative to PSI (ETR_I) indicated the expected linear relationship (*SI Appendix*, Fig. S5). However, when only cytochrome P450 was expressed, ETR_I was elevated relative to ETR_{II}. This indicates that CYP1A1 promotes PSI maximal activity, and has implications for PSI limitations in uninduced cultures (*Discussion*) (36).

Although coexpression of both sinks generally promoted additive effects on photosynthetic performance based on these measurements, we observed potential competition between the introduced pathways. Expression of the sucrose export pathway in strains expressing CYP1A1 led to reduced cytochrome P450 monooxygenase activity (Fig. 3*E*). On the other hand, cytochrome P450 coexpression did not impact total levels of sucrose exported at 100-μmol photons m^{-2} s^{-1}; however, a slight but significant decrease in sucrose exported was observed at intensities >100-μmol photons m^{-2} s^{-1} when cytochrome P450 activity was coinduced (Fig. 3*F*). Sucrose export led to major changes in biomass distribution in the cells (*SI Appendix*, Fig. S6 *A* and *B*), significantly increasing the total biomass accumulated (dry cell mass + exported sucrose) relative to uninduced controls (*SI Appendix*, Fig. S6*C*). Induction of cytochrome P450 activity did not have the same large change in carbon allocation (as expected because it is solely an electron sink), although a slight increase in per cell biomass accumulation was observed with both sinks active (*SI Appendix*, Fig. S6*C*).

Alternative Electron Acceptors Do Not Account for Carbon Sink–Induced Photosynthetic Enhancements. One possible interpretation of the photosynthetic enhancements caused by heterologous sink expression is that the spectroscopic data resulted from an unanticipated increase in activity of natural alternative electron acceptors. We therefore examined the impact of expressing sinks under conditions with disabled alternative electron acceptors. We first tested the elimination of FDPs, a major electron sink downstream of PSI that has been reported to consume ∼20 to 30% of electrons generated from PSII under quasi-steady state in *Synechocystis* sp. PCC 6803 in the 10 to

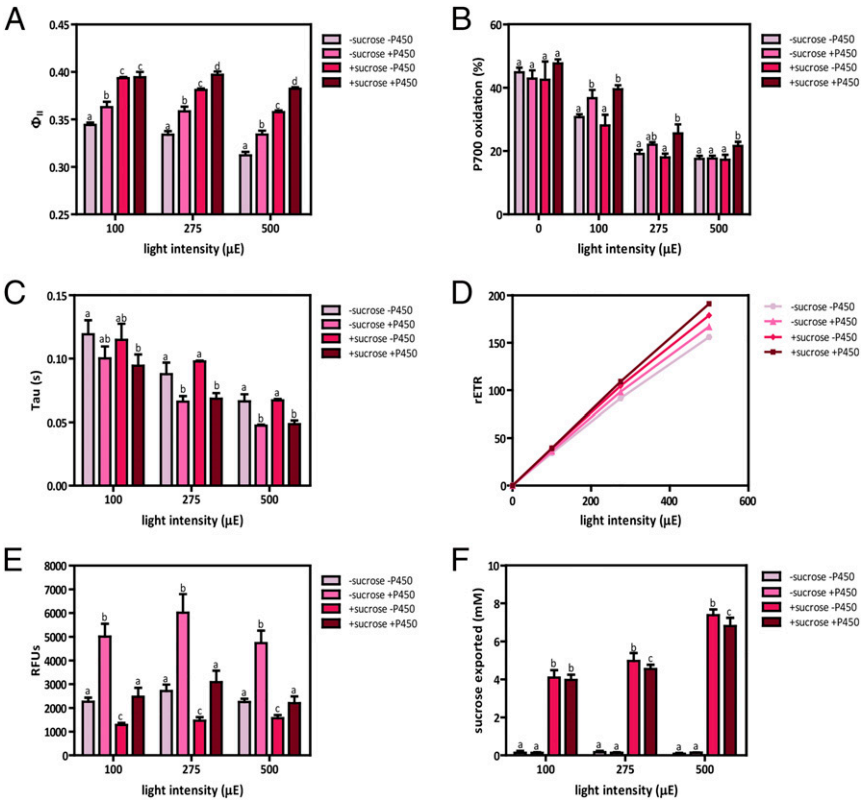

Fig. 3. Simultaneous expression of both sinks has additive effects on photosynthetic capacity. (*A*) Φ_{II} values measured at three different light intensities 24 h after activation of sucrose and/or cytochrome P450 sinks. (*B*) P700 oxidation levels, expressed as a percentage, measured at three different light intensities 24 h after activation of sucrose and/or cytochrome P450 sinks. (*C*) $P700^+$ τ values, expressed in seconds, measured at three different light intensities 24 h after coactivation of both sucrose and cytochrome P450 sinks. (*D*) rETR measured at three different light intensities 24 h after activation of sucrose and/or cytochrome P450 sinks. (*E*) CYP1A1 activity measured at three different light intensities 24 h after of coactivation of both sucrose and cytochrome P450 sinks. (*F*) Sucrose exported levels measured after 24 h of coactivation of both sucrose and cytochrome P450 sinks. CscB/SPS/P450 strain was used for the experiments showed in all panels. Sucrose export was induced by adding 1 mM IPTG to induce *cscB* and *sps* (±sucrose, respectively). Cytochrome P450 activity was induced by addition of 1 mM theophylline to promote *cyp1a1* expression (±P450, respectively). Averages of ≥3 independent biological replicates are shown + SD. Significance was calculated by one-way ANOVA followed by Tukey's multiple comparison test. Bars labeled with different letters are significantly different ($P < 0.05$).

20 min following a dark-to-light transition (37). The genome of *S. elongatus* encodes for two FDPs, Flv1 and Flv3, that function as a heterodimer (11, 38), but lacks the Flv2/4 pair found in some other cyanobacterial species (e.g., *Synechocystis* sp. PCC 6803). The FDP knockout mutants (Δ*flv1/3*) we generated exhibited substantial differences in fluorescence and spectroscopic kinetics compared to a wild-type background (*SI Appendix*, Fig. S7), as reported previously in *Chlamydomonas reinhardtii* (39). Chlorophyll a fluorescence continued to rise throughout the duration of a 1.5-s saturating flash in FDP mutants in comparison to the wild-type (contributing to higher apparent F'_M values measured during saturation pulses), and the relaxation of chlorophyll fluorescence following the flash was substantially slower (*SI Appendix*, Fig. S7). We observed a similar enhancement in Φ_{II} when sucrose export was induced in an FDP knockout (Fig. 4*A* and *SI Appendix*, Fig. S9*A*), suggesting FDP activity cannot account for the improvement in photosynthetic parameters when a sucrose sink is engaged. However, somewhat unexpectedly, knockout of FDPs significantly impacted the photosynthetic enhancements observed following cytochrome P450 expression, decreasing the values of Φ_{II}, especially at low light intensity (Fig. 4*B* and *SI Appendix*, Fig. S9*B*), mostly due to a decrease of F'_M (*SI Appendix*, Fig. S8*A*).

RTOs participate in the ETC of *S. elongatus*, including cytochrome *bd* quinol oxidase (Cyd) and COX, which accept electrons from the plastoquinone and plastocyanin/cytochrome c_6 pools, respectively (6). Relative to FDPs, RTOs are thought to consume only a minor fraction of photosynthetic reductant (~6%) (14) and may not typically play dominant roles in photoprotection, although RTO activity may be up-regulated under certain conditions [e.g., when FDP activity is insufficient to prevent linear electron transport blockage at the level of cytochrome b_6f or PSI (14)]. Addition of 1 mM potassium cyanide (KCN), which is known to inhibit RTOs (40, 41), did not diminish the increase in Φ_{II} observed following sucrose export (Fig. 4*C* and *SI Appendix*, Fig. S9*C*). A similar pattern was observed for cyanide treatment in a Δ*flv1/3* background (*SI Appendix*, Fig. S9*E*). Taken together, these data suggests that inhibition of at least three of the most dominant alternative electron acceptors does not impair the ability of a sucrose sink to enhance photosynthesis. Similarly, the addition of KCN did not impact the gain in photosynthetic efficiency obtained by the activity of cytochrome P450 at ≤275-µmol photons m^{-2} s^{-1} intensities (Fig. 4*D* and *SI Appendix*, Fig. S9*D*), but not at 500-µmol photons m^{-2} s^{-1}, where Φ_{II} decreases due to a decrease of F'_M (*SI Appendix*, Fig. S8*B*), indicating that RTOs are not involved in the increase in Φ_{II} observed after CYP1A1 expression. Furthermore, KCN treatment did not exacerbate the loss of Φ_{II} caused by CYP1A1 expression in FDP knockout strains (*SI Appendix*, Fig. S9*F*).

The apparent competition between heterologous sinks for electrons from PSI seen in the above results prompted us to

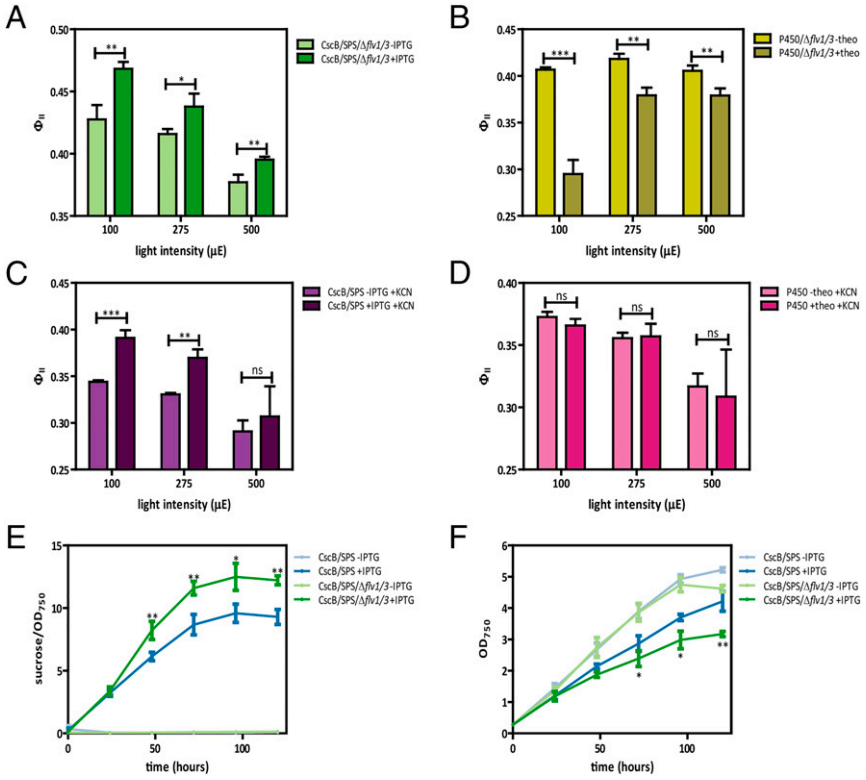

Fig. 4. The nature of the heterologous sink influences its competition with endogenous sinks. (*A* and *B*) Φ_{II} values in absence of FDPs measured at three different light intensities 24 h after activation of sucrose sink (*A*) or cytochrome P450 sink (*B*). (*C* and *D*) Φ_{II} values in absence of RTOs (activity blocked with KCN) measured at three different light intensities 24 h after activation of sucrose sink (*C*) or cytochrome P450 sink (*D*). (*E*) Sucrose exported per OD_{750} unit at different time points following induction of *cscB* and *sps* genes by IPTG in the presence/absence of FDPs (Δ*flv1/3*). (*F*) Cell growth of cultures shown in *E* at different time points following induction of *cscB* and *sps* genes by IPTG in the presence/absence of FDPs (Δ*flv1/3*). Averages of ≥3 independent biological replicates are shown ± SD. Significance was calculated by unpaired Student's *t* test relative to uninduced strain as control; $*P < 0.05$, $**P < 0.01$, $***P < 0.001$; ns, not significant. *A–E* are by one-way ANOVA followed by Tukey's multiple comparison test. Bars labeled with different letters are significantly different ($P < 0.05$) (*F*). An extended version of *A–D* can be found in *SI Appendix*, Fig. S9 *A–D*, respectively.

investigate if heterologous sinks compete with natural photoprotective sinks. We first examined sucrose export capacity in cells with and without FPDs. Sucrose export was enhanced on a per cell basis in the Δ*flv1/3* background (Fig. 4*E* and *SI Appendix*, Fig. S1*A*), albeit at the expense of growth rate (Fig. 4*F*). This provides indirect evidence that endogenous FDP activity may compete for reductant that could otherwise be used for bioproduction and biomass formation, potentially even under constant moderate illumination (i.e., 150-µmol photons m^{-2} s^{-1}). These results demonstrated the existence of an interconnection between biomass formation, PSI oxidation, and sucrose production. The highest rates of biomass accumulation (both total

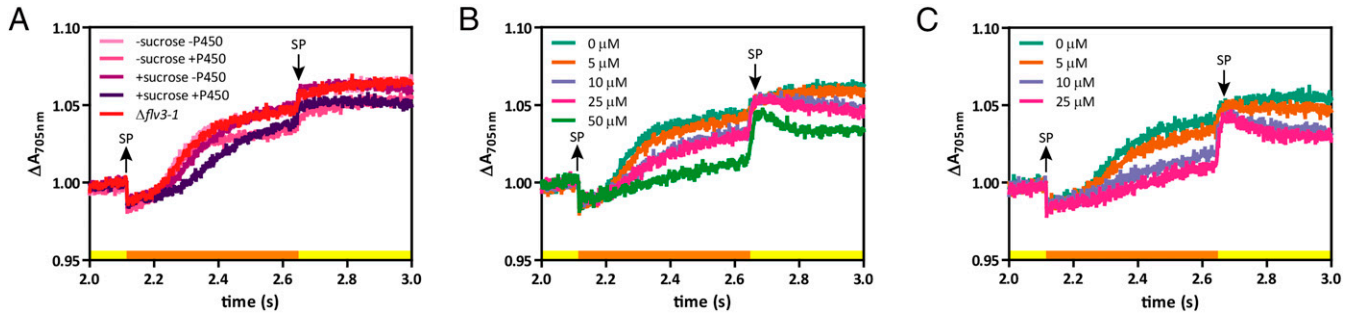

Fig. 5. Heterologous sinks can partially compensate for PSI overreduction caused by fluctuating light conditions. (*A*) Redox kinetics of P700 during a saturation pulse measured after 24 h of coactivation of sucrose and cytochrome P450 sinks individually and together in a strain lacking the protective FDP proteins (CscB/SPS/P450/Δ*flv1/3*). (*B* and *C*) Redox kinetics of P700 during a saturation pulse in presence of different concentrations of BV measured after 24 h in a strain lacking the protective FDP proteins without (*B*) and with (*C*) coactivation of both sucrose and cytochrome P450 sinks. CscB/SPS/P450/Δ*flv1/3* strain was used for the experiments showed in all panels. Sucrose export was induced by adding 1 mM IPTG to induce *cscB* and *sps* (±sucrose, respectively). Cytochrome P450 activity was induced by addition of 1 mM theophylline to promote *cyp1a1* expression (±P450, respectively). Averages of ≥3 independent biological replicates are shown. P700 kinetic measurements were taken with 500-µmol photons m^{-2} s^{-1} of blue actinic light (yellow boxes). Saturation pulses (SP) of ∼0.5 s (orange boxes) were applied to promote complete oxidation of P700 and were turned on at the time point indicated by upward arrows and off at the time point indicated by a downward arrow.

biomass and on a per cell basis) were observed in strains expressing both heterologous sinks within a Δ*flv1/3* background (*SI Appendix*, Fig. S6*C*). On the other hand, cytochrome P450 activity was not impacted by the removal of FDPs (*SI Appendix*, Fig. S1*C*). Taken together, these data show that heterologous sucrose export significantly enhanced photosynthetic performance under our culture conditions (Fig. 2*A*) in a manner that was independent of endogenous water–water mechanisms (Fig. 4 *A* and *C* and *SI Appendix*, Fig. S9 *C* and *D*), whereas cytochrome P450 expression had moderate photosynthetic effects (Fig. 2*B*) that were more pronounced under high light (Fig. 2*A*), which may be linked to the activity of natural sinks (e.g., FDPs) (Fig. 4*B* and *SI Appendix*, Fig. S9*B*).

Heterologous Sinks Can Partially Compensate for the Loss of PSI Oxidation Mechanisms. The observation of increased rETR (Fig. 3*D*) and higher P700 oxidation levels (Fig. 3*B*) suggested that both heterologous sinks act as efficient acceptors of reductant from PSI, and thus may partially compensate for a loss of FDPs (11). As reported previously in cyanobacteria (42) and algae (43), the lack of the protective FDP proteins impaired the ability of *S. elongatus* to maintain an oxidized PSI pool during a transient pulse of saturating light (*SI Appendix*, Fig. S10). Expressing one of the two sinks had a minor effect on P700 oxidation kinetics in a strain lacking FDPs (Fig. 5*A*), but when both sinks were simultaneously activated, the kinetics of PSI reduction were significantly slowed (Fig. 5*A*). This improvement in $P700^+$ levels was correlated with sucrose production and export, but was not observed upon supplementation with extracellular (exogenous) sucrose (*SI Appendix*, Fig. S11). A similar effect was observed in Φ_{II} levels, where the presence of exogenous sucrose has a negative impact (100-μmol photons m^{-2} s^{-1}) or no significant effect (≥275-μmol photons m^{-2} s^{-1}) regardless of cytochrome P450 activation (*SI Appendix*, Fig. S12). These results were consistent across all tested light conditions (*SI Appendix*, Fig. S13 *A* and *D*), although the heterologous sinks were not sufficient to recover the fully oxidized PSI pool under fluctuating light.

To test if the changes in P700 oxidation were due to a partial mitigation of excess reductant building up on PSI, we supplemented cells with benzyl viologen (BV), an artificial electron acceptor capable of accepting electrons from PSI. First, we verified that titrating BV into FDP knockout mutants was able to eliminate the acceptor side limitation of PSI and restore an oxidized PSI pool during a saturating pulse. Addition of 50 μM BV was required to completely rescue the P700 oxidation kinetics during a saturating light pulse in Δ*flv1/3* cells without activated sinks (Fig. 5*B*). However, when both sinks were activated in this background, 10 μM BV was sufficient to recover wild-type–like oxidation kinetics during a saturating light pulse (Fig. 5*C*), suggesting that sucrose export and cytochrome P450 sinks were mitigating a substantial proportion of reductant building up on the PSI acceptor side during a light transient. These results were consistent across all steady-state light conditions analyzed (*SI Appendix*, Figs. S13 *B*, *C*, *E*, and *F*).

Discussion

Taken together, our results demonstrate the expression of heterologous sinks have a positive effect on photosynthetic performance, and are broadly consistent with an emerging phenomenon of many different heterologous bioproduction metabolic pathways that can impart photosynthetic benefits in engineered cyanobacterial strains (44). One parsimonious hypothesis for these effects is that heterologous metabolic sinks may capitalize on excess potential energy in the ETC, providing an outlet for captured energy that might otherwise be directed toward photoprotective systems or other "release valves," although this theory would have interesting implications for cyanobacterial metabolism. We show that two different sinks when operated individually lead to enhanced photosynthetic performance, although the effects are not identical and may depend on the nature of the sink introduced. Furthermore, activating these sinks simultaneously can lead to additive photosynthetic improvements, especially at high light intensities where cytochrome P450 activities are more pronounced (≥275-μmol photons m^{-2} s^{-1}). We find that many such photosynthetic improvements cannot be explained simply as an effect of upregulated native sinks. Indeed, heterologous metabolism may be capable of substituting for some PSI oxidizing activities, albeit to a limited extent.

Our data validate and expand upon recent reports of improved photosynthesis in cyanobacteria engineered with carbon heterologous sinks [e.g., sucrose (16, 17), 2,3-butanediol (18), isoprene (19), and glycerol (20)]. In particular, we corroborate the positive effect on multiple photosynthetic parameters observed following expression of a sucrose export, including improved PSII activity (Figs. 2*A* and 3*A*). An increase in the photosynthetic efficiency was also observed when we explored the impact of an electron sink, the cytochrome P450 CYP1A1, similar to observations when this gene was expressed in *Synechococcus* sp. PCC 7002 (21, 22). Expression of cytochrome P450 sink leads to enhancements in quantum yield of PSII, electron turnover time in PSI and P700 oxidation levels (Fig. 2 *B*–*D*), demonstrating that this is not a species-specific effect. We also find that a number of the sink-dependent photosynthetic enhancements we observed are maintained after eliminating the activity of endogenous alternative electron acceptors (FDPs and RTOs) (Fig. 4 and *SI Appendix*, Fig. S9), indicating that the changed photosynthetic parameters are not the result of increased engagement of energy-consuming mechanisms. Conversely, eliminating the water–water cycle catalyzed by Flv1/3 can enhance the yield of sucrose on a per cell basis under some of the conditions we tested (Fig. 4 *A* and *E* and *SI Appendix*, Figs. S6 and S9*A*). This is broadly consistent with recent reports that FDP inactivation increases poly-β-hydroxybutyrate and glycogen production in *Synechocystis* sp. PCC 6803 (45) or H_2 production in *C. reinhardtii* (46, 47), although it remains to be definitively demonstrated if this is a direct effect of redirecting photosynthetic electron flux that would have otherwise been consumed by Flv1/3. For example, since water–water cycles contribute to the generation of proton motive force (and ATP generation), other alterations in energy balance likely occur when flux to such pathways is restricted which could influence bioproduction pathways.

More surprisingly, we showed that combining more than one heterologous sink in the same strain shows additive effects in the photosynthetic efficiency of PSII (Fig. 3*A*) and P700 oxidation levels (Fig. 3*B*). These results provide support for the hypothesis that neither sink alone is capable of utilizing the full overcapacity of the ETC. However, there are indications of diminishing returns with additional sinks, and we find evidence that there is competition between two heterologous sinks (Fig. 3*E*). This observation is conceptually similar with other reports in the literature, such as in *C. reinhardtii* cells, where the Calvin–Benson cycle has been shown to "outcompete" the hydrogenase, HydA, for electrons, thereby hindering H_2 production (47–50). Currently, it is unclear why CPYA1's activity seems to activate predominately at higher light intensities in comparison to the heterologous sucrose export pathway. However, this may suggest that CYP1A1 activity is linked to the saturation of downstream processes such as carbon fixation.

Photosynthetic improvements observed upon expression of cytochrome P450 were mainly concentrated around PSI—for example, decrease in τ (Figs. 2*C* and 3*C*), increase in P700 oxidation levels (Figs. 2*D* and 3*B*), and preferential ETR_I increases (*SI Appendix*, Fig. S5)—although enhancements in Φ_{II} were observed particularly at higher illumination intensities. The

preferential enhancement under high illumination suggests that cytochrome P450 may be acting as a heterologous dissipation valve and increasing the illumination at which photosynthesis is saturated, consistent with work in other cyanobacterial species. The beneficial effects of activating sucrose export were more pronounced in parameters related to PSII activities (e.g., increase in Φ_{II} levels) (Figs. 2*A* and 3*A*). These observations are intriguing, and may prove to be related to the distinctions between the type of metabolic sink that each of these pathways represent (i.e., cytochrome P450 primarily consumes reducing potential while sucrose export consumes fixed carbon, requiring ATP and NADPH). Another unexpected result that may be related to this is our observation that chlorophyll fluorescence kinetics (associated largely with PSII) were substantially altered in Δ*flv1/3* strains where cytochrome P450 was induced, especially at low light (Fig. 4*B* and *SI Appendix*, Figs. S8 and S9*B*). It might be naïvely expected that cytochrome P450 activity could be better suited to replace Flv1/3 activity, as they both utilize reductant from the acceptor side of PSI, although FDP activity is finely regulated in response to the status of the ETC, while heterologous enzymes are not sophisticatedly integrated into the photosynthetic system. One speculative possibility is that cytochrome P450 activity may exacerbate ATP/NADPH imbalances caused by elimination of dissipative water–water cycles, and this may be more problematic under some illumination regimes than others. Further analysis of the physiological and regulatory responses related to these distinct metabolic sinks would be critical for maximizing realized gains in photosynthetic efficiency, and sustaining them over long-term cultivations.

We demonstrate that these heterologous sinks may partially compensate for the loss of the PSI oxidation mechanisms even under rapid illumination changes (Fig. 5), mitigating accumulation of electrons at the acceptor side of PSI. The same phenomenon has been recently reported in *C. reinhardtii*, where H_2 photoproduction was able to compensate for the loss of FDPs, but only during steady-state conditions (46). Although we find the heterologous sinks are insufficient to fully replace the activity of Flv1/3, this is an intriguing observation with implications for the stability of engineered metabolic circuits in real-world applications. The inability of the heterologous sinks we examined to totally replace the function that FDPs performed could be explained in several possible ways. O_2 photoreduction catalyzed by FDPs has a fast induction after exposure to high flashing-light frequencies (39, 51), whereas there is no inbuilt regulation to enhance the activity of either heterologous sink under certain conditions: Indeed, Calvin–Benson cycle activation may be delayed relative to changes in irradiation (52). Localization of the respective pathways may also play a critical role: Whereas FDPs are soluble enzymes thought to be dynamically regulated to rapidly quench excess NADPH (43), the localization of cytochrome P450 has not been rigorously tested under heterologous conditions, though it is suspected to be membrane-anchored, which could reduce the speed of its activity to accept electron flow from PSI.

Increasing the capacity of heterologous metabolism to efficiently accept electrons from PSI could be an area for future improvement (53). Genetic fusions could be employed for the coupling of sink acceptors to PSI. A number of analogous fusions have been reported to increase electron transfer in the literature, including cytochrome P450 fusion to PsaM (54) or Fd (53, 55), or hydrogenase fusion to PsaC (56), PsaD (57), PsaE (58), or Fd (59). Reducing the affinity of FNR (Fd-$NADP^+$-oxidoreductase) interaction by point mutations could be used as strategy to redirect photosynthetic electrons through heterologous production pathways (60). Rationally designing engineered metabolic pathways could be used to generate heterologous sinks more responsive to dynamic conditions, analogous to natural sinks. This also could help to increase the stability of heterologous pathways, effectively creating a selective pressure and reducing the metabolic burden in the engineered strains. Laboratory evolution might offer an interesting approach to improve the capacity of heterologous sinks to act as photoprotective mechanisms (61, 62).

Given the observations above, it is interesting to consider what endogenous pathways limit cyanobacterial photosynthetic utilization. The fact that multiple cyanobacterial species appear to be able to up-regulate photosynthetic activity to "match" an increased metabolic burden implies that other factors required for growth may be rate-limiting or that their metabolism is regulated to underutilize the full potential of their photosynthetic productivity. Indeed, we find a capacity to fix a significantly higher amount of biomass is unveiled when both heterologous sinks are activated relative to uninduced controls (*SI Appendix*, Fig. S6). Since the potential to increase photosynthetic activity and/or carbon fixation are inherent within the system, then either: 1) the cells could be operating below their "highest potential" metabolic rate; or 2) the light reactions and light capture are not sufficiently tuned down to better match metabolism. This dichotomy between photosynthetic potential and captured energy utilization has important implications for bioproductivity and bioengineering.

Overall, our work provides additional support for the hypothesis that activation of heterologous metabolic sinks can act to improve photosynthetic efficiencies in part by utilizing excess energy transiently captured by photosynthetic machinery under sink-limiting conditions. The concept of "sink engineering" for improving photosynthetic efficiency is akin to, but distinct from, other strategies for source/sink engineering, such as truncation of the light-harvesting antenna (63, 64). If heterologous metabolic circuits can be suitably programmed to be dynamically regulated in response to energetic inputs, it is theoretically possible that they could be used to conserve some of the large amount of total reducing equivalents that can be otherwise directed toward energy-quenching photoprotective processes [up to 90% under some environmental conditions (65, 66)]. However, fully realizing the potential of sink engineering in cyanobacteria and algae will require more fundamental research into the molecular mechanisms used to sense and poise source/sink energy balance in unicellular photosynthetic microbes. Such mechanisms are beginning to be uncovered in microalgae (67), but remain relatively undiscovered in cyanobacteria (44).

Materials and Methods

Strains and Culture Conditions. All strains used in this study are listed in *SI Appendix*, Table S1 and described in *SI Appendix*, Fig. S14. *S. elongatus* was grown in a Multitron incubator (Infors HT) at 32 °C and supplemented with 2% CO_2 with ~150-μmol photons m^{-2} s^{-1} of light provided by Sylvania 15 W Gro-Lux fluorescent bulbs. Cultures were shaken at 150 rpm in BG11 supplemented with 1 g L^{-1} Hepes to a final pH of 8.3 with NaOH. Cultures were back-diluted daily to an OD_{750} of 0.3 and acclimated to the medium/irradiance for at least 3 d prior to experiments or IPTG induction. Where appropriate, 1 mM IPTG or 1 mM theophylline was added to induce *cscB* and *sps* gene expression or *cyp1a1* gene expression, respectively. Chloramphenicol (Cm; 25 μg mL^{-1}), Kanamycin (Kn; 50 μg mL^{-1}), and Spectinomycin (Sp; 100 μg mL^{-1}) were used to maintain *cscB*-, *sps*-, and *cyp1a1*-containing cells, respectively. Gentamicin (Gm; 2 μg mL^{-1}) was used to maintain the FDP inactivation mutant Δ*flv1/3*. In all cases, antibiotic selection was removed prior to conducting any of the reported experiments to minimize any unintended effects.

Strain Construction. *S. elongatus* with genomically integrated copies of *cscB* and *sps* under an IPTG-inducible promoter were previously described (16). The gene sequence for *cyp1a1*, as described in Berepiki et al. (22) (pSy21), was cloned into NS1 (pSyn_1/D-TOPO; Thermo Fisher Scientific) modified with an upstream theophylline-responsive riboswitch together with a *conII* promoter (27). Genomic loci encoding FPDs were disrupted by inserting a gentamicin-resistance cassette. We confirmed the insertion of all these

PLANT BIOLOGY

constructs in the genome of *S. elongatus* by PCR. Plasmid details are reported in *SI Appendix*, Table S2.

Sucrose Quantification. Secreted sucrose was quantified from supernatants using the Sucrose/D-Glucose Assay Kit (K-SUCGL; Megazyme), and converted into cell basis via OD_{750} standard curve calibration.

Dry Cell Weight Measurement. Dry cell mass was determined as previously described with some modifications (68). *S. elongatus* cultures (~45 mL) were harvested after 24 h postinduction by centrifugation at 4,000 rpm for 30 min. Pellets were washed twice with distillated water and transferred onto cellulose acetate membranes (0.45 μm; Whatman) and immediately dried in a stove for ≥4 h at 90 °C. The mass of each membrane was measured with an analytical balance before and after adding the cells, and these data were used to calculate the dry cell weight per volume.

EROD Assay for Cytochrome P450 Activity. CYP1A1 activity was measured using an EROD assay, as described previously (22). Briefly, cells from an exponentially growing culture were adjusted to $OD_{750} = 0.1$ with BG11 medium and 100-μL suspension was dispensed in triplicate to a black 96-well microplate (Grenier Bio-One) and allowed to equilibrate for 10 min under standard growth conditions. Then, 100 μL of BG11 containing 5 μM 7-ethoxyresorufin was added to each well, and the fluorescent product resorufin was monitored via microplate reader (excitation 544 nm, emission 590 nm; Fluostar Optima by BMG Labtech).

Fluorescence Measurements. Quantum yield of PSII (Φ_{II}) measurements were performed on a custom-built fluorimeter/spectrophotometer (69) modified for liquid samples by using a cuvette holder with a pulsed measuring beam (590-nm peak emission light-emitting diode [LED], Luxeon Z Color Line). The sample was then illuminated at three different intensities of photosynthetically active radiation (PAR), 100-, 275-, and 500-μmol photons m^{-2} s^{-1} (460-nm peak emission; Luxeon Rebel Royal-Blue LED). Before the first saturating pulse, and between each pulse, the cuvette was illuminated at the relevant actinic light for 3 min and 2 min, respectively, to acclimate the sample and minimize the impact of successive saturating pulses. Chlorophyll fluorescence was filtered with a long-pass RG 695-nm filter in front of the detector. Samples containing cyanobacteria (2.5 μg mL^{-1} chlorophyll) resuspended in fresh medium sparged with 2% CO_2 in air were dark-adapted for 3 min before measuring. The relative yields of chlorophyll fluorescence were measured under steady-state illumination (F_s), during a 1.5-s saturating pulses of actinic light (~5,000-μmol photons m^{-2} s^{-1}) (F'_M) and after exposure to ~2 s of darkness with far red illumination (F'_0). Chlorophyll fluorescence was used to calculate Φ_{II} and the coefficient of photochemical quenching (q_p) (29). The following equations were used $\Phi_{II} = (F'_M - F_s)/(F'_M)$ and $q_p = (F'_M - F_s)/(F'_M - F'_0)$, where F'_M is the value of maximal fluorescence in the light-adapted state, F_s is the steady-state fluorescence in the light-adapted state, and F'_0 is the minimal fluorescence in the light-adapted state. rETR was calculated as the product of Φ_{II} and PAR (70). Where applicable, KCN was added to a final concentration of 1 mM.

PSI Absorbance Changes. To evaluate P700 redox changes, samples were monitored semisimultaneously with fluorescence measurements, using the instrument described in Hall et al. (69) by measuring absorbance changes at about 703 nm. The measuring beam was generated by a pulsed LED (720-nm peak emission; Rebel LUXEON Far Red) filtered with a 5-nm band-pass filter centered at 700 nm, resulting in a measured emission peak at ~703 nm (16). The signals were detected with a photodiode (69) filtered with a Schott RG-695 filter to block actinic light. The sample was illuminated at three different intensities of PAR, 100-, 275-, and 500-μmol photons m^{-2} s^{-1} (460-nm peak emission; Luxeon Rebel Royal-Blue LED) for 3 min prior to every saturating pulse analysis. Samples containing cyanobacteria cells were prepared by resuspended cells in fresh medium to a concentration of 5 μg mL^{-1} chlorophyll and sparged with 2% CO_2 in air. Samples were dark-adapted for 3 min before starting measurements. The percentage of oxidized P700 was calculated as $[(P_{ox} - P_{ss})/(P_{red} - P_{ox})] \times 100$, where P_{ox} was the maximum extent of P700 absorbance signal induced by a saturating pulse of light during ~0.5 s (~5,000-μmol photons m^{-2} s^{-1}); P_{ss}, taken to be the fraction of $P700^+$ in under steady-state illumination, estimated by the extent of P700 absorbance signal induced by a short dark interval, and assuming that P700 reaches full reduction; and P_{red} is the level of P700 reduced in the dark. PSI traces were normalized to the last point of the steady-state level of oxidation (P_{ss}).

DIRK Absorbance Changes. Steady-state levels of photooxidized P700 ($P700^+$) were estimated by DIRK analysis (32), after 21 s of actinic illumination at three different intensities (100-, 275-, and 500-μmol photons m^{-2} s^{-1}). Samples containing cyanobacteria (2.5 μg mL^{-1} chlorophyll) resuspended in fresh medium containing 2% CO_2 and were dark-adapted for 3 min before measuring. The half-time of $P700^+$ rereduction (τ), was measured from the absorbance change at 703 nm (ΔA_{703}) during a dark interval of 2,100 ms; τ was calculated by the monotonic decay kinetic of ΔA_{703} produced after extinguishing the actinic light (71), whereas that the velocity of $P700^+$ rereduction (V_{in}) was calculated as the quotient of the amplitude (A) of this decay divided by τ ($V_{in} = A/\tau$).

Detection of CYP1A1 by Western Blotting. *S. elongatus* whole-cell extracts were prepared as described previously (22), with minor modifications. Cells were disrupted using a tissue lyser (Qiagen) with zirconium beads (0.1 mm; Biospec Products) for two cycles of 30 s at a frequency of 30 Hz. After centrifugation, the supernatants were used to determine protein concentration by the BCA method using bovine serum albumin (BSA) as a standard. Next, 30 μg of total protein was separated in a Bis-Tris NuPAGE gel and transferred to a 0.45-μm polyvinyl fluoride (PVDF) membrane using a transfer apparatus according to the manufacturer's protocols (Invitrogen). After incubation with blocking solution (TBS-T; 20 mM Tris-Cl, 150 mM NaCl, 0.02% [vol/vol] Tween-20, pH 7.6 supplemented with 2% [wt/vol] ECL Advance blocking reagent; GE Healthcare) for 1 h, the membrane was washed once, and incubated with mouse monoclonal anti-FLAG M2-peroxidase (HRP) antibody (Sigma; 1:1000). Membranes were washed three times for 5 min in TBS-T then developed with the SuperSignal West Dura (Thermo Scientific) ECL system and imaged using a Versa-Doc Imaging system (Bio-Rad).

Statistical Analysis. Recorded measurements are represented as mean values, with error bars expressing the SD of $n \geq 3$ biological replicates experiments, as indicated. The significance of differences between groups was evaluated by one-way ANOVA followed by Tukey's multiple comparison test or by an unpaired Student's t test. Statistical analyses were carried out using GraphPad Prism software (GraphPad Software). Differences were considered statistically significant at $P < 0.05$.

Data Availability. All study data are included in the article and *SI Appendix*.

ACKNOWLEDGMENTS. We thank Dr. Robert Zegarac for his assistance with technical matters related to spectroscopy instrumentation. Molecular biology and spectroscopic studies performed in the laboratory of D.C.D. were supported by DE-FG02-91ER20021, awarded from the Photosynthetic Systems program of the Division of Chemical Sciences, Geosciences, and Biosciences, Office of Basic Energy Sciences of the US Department of Energy. Additional spectroscopic studies were supported in the laboratory of D.M.K. by DE-FG02-91ER20021. Biochemical assays and spectroscopy performed in the laboratory of T.S.B. were supported by the Biotechnology and Biological Sciences Research Council (Grant BB/P019331/1). In addition, a portion of D.M.K.'s salary is supported by Michigan State University AgBioResearch.

1. L. Al-Haj, Y. T. Lui, R. M. Abed, M. A. Gomaa, S. Purton, Cyanobacteria as chassis for industrial biotechnology: Progress and prospects. *Life (Basel)* **6**, 6 (2016).
2. A. Melis, Solar energy conversion efficiencies in photosynthesis: Minimizing the chlorophyll antennae to maximize efficiency. *Plant Sci.* **177**, 272–280 (2009).
3. B. L. Montgomery, The regulation of light sensing and light-harvesting impacts the use of cyanobacteria as biotechnology platforms. *Front. Bioeng. Biotechnol.* **2**, 22 (2014).
4. S. A. Johansson *et al*., Isolation and molecular characterisation of *Dunaliella tertiolecta* with truncated light-harvesting antenna for enhanced photosynthetic efficiency. *Algal Res.* **48**, 101917 (2020).
5. M. Santos-Merino, A. K. Singh, D. C. Ducat, New applications of synthetic biology tools for cyanobacterial metabolic engineering. *Front. Bioeng. Biotechnol.* **7**, 33 (2019).
6. D. J. Lea-Smith, P. Bombelli, R. Vasudevan, C. J. Howe, Photosynthetic, respiratory and extracellular electron transport pathways in cyanobacteria. *Biochim. Biophys. Acta* **1857**, 247–255 (2016).
7. J. B. Vicente, C. M. Gomes, A. Wasserfallen, M. Teixeira, Module fusion in an A-type flavoprotein from the cyanobacterium *Synechocystis* condenses a multiple-component pathway in a single polypeptide chain. *Biochem. Biophys. Res. Commun.* **294**, 82–87 (2002).
8. L. Nikkanen *et al*., Functional redundancy between flavodiiron proteins and NDH-1 in Synechocystis sp. PCC 6803. *Plant J.* **103**, 1460–1476 (2020).
9. G. Brändén, R. B. Gennis, P. Brzezinski, Transmembrane proton translocation by cytochrome c oxidase. *Biochim. Biophys. Acta* **1757**, 1052–1063 (2006).
10. C. W. Mullineaux, Co-existence of photosynthetic and respiratory activities in cyanobacterial thylakoid membranes. *Biochim. Biophys. Acta* **1837**, 503–511 (2014).

11. Y. Allahverdiyeva *et al*., Flavodiiron proteins Flv1 and Flv3 enable cyanobacterial growth and photosynthesis under fluctuating light. *Proc. Natl. Acad. Sci. U.S.A.* **110**, 4111–4116 (2013).
12. D. J. Lea-Smith *et al*., Thylakoid terminal oxidases are essential for the cyanobacterium *Synechocystis* sp. PCC 6803 to survive rapidly changing light intensities. *Plant Physiol.* **162**, 484–495 (2013).
13. G. Shimakawa, C. Miyake, Respiratory terminal oxidases alleviate photo-oxidative damage in photosystem I during repetitive short-pulse illumination in *Synechocystis* sp. PCC 6803. *Photosynth. Res.* **137**, 241–250 (2018).
14. M. Ermakova *et al*., Distinguishing the roles of thylakoid respiratory terminal oxidases in the cyanobacterium *Synechocystis* sp. PCC 6803. *Plant Physiol.* **171**, 1307–1319 (2016).
15. Y. Helman *et al*., Genes encoding A-type flavoproteins are essential for photoreduction of O_2 in cyanobacteria. *Curr. Biol.* **13**, 230–235 (2003).
16. B. W. Abramson, B. Kachel, D. M. Kramer, D. C. Ducat, Increased photochemical efficiency in cyanobacteria via an engineered sucrose sink. *Plant Cell Physiol.* **57**, 2451–2460 (2016).
17. D. C. Ducat, J. A. Avelar-Rivas, J. C. Way, P. A. Silver, Rerouting carbon flux to enhance photosynthetic productivity. *Appl. Environ. Microbiol.* **78**, 2660–2668 (2012).
18. J. W. K. Oliver, S. Atsumi, A carbon sink pathway increases carbon productivity in cyanobacteria. *Metab. Eng.* **29**, 106–112 (2015).
19. X. Gao *et al*., Engineering the methylerythritol phosphate pathway in cyanobacteria for photosynthetic isoprene production from CO_2. *Energy Environ. Sci.* **9**, 1400–1411 (2016).
20. P. Savakis *et al*., Photosynthetic production of glycerol by a recombinant cyanobacterium. *J. Biotechnol.* **195**, 46–51 (2015).
21. A. Berepiki, J. R. Gittins, C. M. Moore, T. S. Bibby, Rational engineering of photosynthetic electron flux enhances light-powered cytochrome P450 activity. *Synth. Biol. (Oxf.)* **3**, ysy009 (2018).
22. A. Berepiki, A. Hitchcock, C. M. Moore, T. S. Bibby, Tapping the unused potential of photosynthesis with a heterologous electron sink. *ACS Synth. Biol.* **5**, 1369–1375 (2016).
23. S. B. Mellor, K. Vavitsas, A. Z. Nielsen, P. E. Jensen, Photosynthetic fuel for heterologous enzymes: The role of electron carrier proteins. *Photosynth. Res.* **134**, 329–342 (2017).
24. D. A. Russo, J. A. Z. Zedler, P. E. Jensen, A force awakens: Exploiting solar energy beyond photosynthesis. *J. Exp. Bot.* **70**, 1703–1710 (2019).
25. T. Yamada *et al*., Enhancement of metabolizing herbicides in young tubers of transgenic potato plants with the rat CYP1A1 gene. *Theor. Appl. Genet.* **105**, 515–520 (2002).
26. H. Kawahigashi, S. Hirose, H. Ohkawa, Y. Ohkawa, Transgenic rice plants expressing human CYP1A1 remediate the triazine herbicides atrazine and simazine. *J. Agric. Food Chem.* **53**, 8557–8564 (2005).
27. A. T. Ma, C. M. Schmidt, J. W. Golden, Regulation of gene expression in diverse cyanobacterial species by using theophylline-responsive riboswitches. *Appl. Environ. Microbiol.* **80**, 6704–6713 (2014).
28. N. R. Baker, Chlorophyll fluorescence: A probe of photosynthesis in vivo. *Annu. Rev. Plant Biol.* **59**, 89–113 (2008).
29. K. Maxwell, G. N. Johnson, Chlorophyll fluorescence—A practical guide. *J. Exp. Bot.* **51**, 659–668 (2000).
30. D. Campbell, V. Hurry, A. K. Clarke, P. Gustafsson, G. Oquist, Chlorophyll fluorescence analysis of cyanobacterial photosynthesis and acclimation. *Microbiol. Mol. Biol. Rev.* **62**, 667–683 (1998).
31. K. Oxborough, N. R. Baker, Resolving chlorophyll a fluorescence images of photosynthetic efficiency into photochemical and non-photochemical components – calculation of q_P and F_v'/F_m' without measuring F_o'. *Photosynth. Res.* **54**, 135–142 (1997).
32. C. A. Sacksteder, D. M. Kramer, Dark-interval relaxation kinetics (DIRK) of absorbance changes as a quantitative probe of steady-state electron transfer. *Photosynth. Res.* **66**, 145–158 (2000).
33. G. Bernát, J. Appel, T. Ogawa, M. Rögner, Distinct roles of multiple NDH-1 complexes in the cyanobacterial electron transport network as revealed by kinetic analysis of $P700^+$ reduction in various Ndh-deficient mutants of *Synechocystis* sp. strain PCC6803. *J. Bacteriol.* **193**, 292–295 (2011).
34. G. Shimakawa, C. Miyake, Oxidation of P700 ensures robust photosynthesis. *Front. Plant Sci.* **9**, 1617 (2018).
35. S. C. Holland *et al*., Impacts of genetically engineered alterations in carbon sink pathways on photosynthetic performance. *Algal Res.* **20**, 87–99 (2016).
36. S. Sello, A. Meneghesso, A. Alboresi, B. Baldan, T. Morosinotto, Plant biodiversity and regulation of photosynthesis in the natural environment. *Planta* **249**, 1217–1228 (2019).
37. Y. Allahverdiyeva, J. Isojärvi, P. Zhang, E. M. Aro, Cyanobacterial oxygenic photosynthesis is protected by flavodiiron proteins. *Life (Basel)* **5**, 716–743 (2015).
38. B. E. Rubin *et al*., High-throughput interaction screens illuminate the role of c-di-AMP in cyanobacterial nighttime survival. *PLoS Genet.* **14**, e1007301 (2018).
39. F. Chaux *et al*., Flavodiiron proteins promote fast and transient O_2 photoreduction in *Chlamydomonas*. *Plant Physiol.* **174**, 1825–1836 (2017).
40. T. Mogi, H. Miyoshi, Properties of cytochrome *bd* plastoquinol oxidase from the cyanobacterium *Synechocystis* sp. PCC 6803. *J. Biochem.* **145**, 395–401 (2009).
41. C. Büchel, O. Zsíros, G. Garab, Alternative cyanide-sensitive oxidase interacting with photosynthesis in *Synechocystis* PCC 6803. Ancestor of the terminal oxidase of chlororespiration? *Photosynthetica* **35**, 223–231 (1998).
42. P. Ilík *et al*., Alternative electron transport mediated by flavodiiron proteins is operational in organisms from cyanobacteria up to gymnosperms. *New Phytol.* **214**, 967–972 (2017).
43. M. Jokel, X. Johnson, G. Peltier, E. M. Aro, Y. Allahverdiyeva, Hunting the main player enabling Chlamydomonas reinhardtii growth under fluctuating light. *Plant J.* **94**, 822–835 (2018).
44. M. Santos-Merino, A. K. Singh, D. C. Ducat, "Sink engineering in photosynthetic microbes" in *Cyanobacteria: Metabolic Engineering and Biotechnology*, E. P. Hudson, Ed. (Wiley, 2021).
45. K. Thiel *et al*., Redirecting photosynthetic electron flux in the cyanobacterium *Synechocystis* sp. PCC 6803 by the deletion of flavodiiron protein Flv3. *Microb. Cell Fact.* **18**, 189 (2019).
46. A. Burlacot *et al*., Flavodiiron-mediated O2 photoreduction links H2 production with CO2 fixation during the anaerobic induction of photosynthesis. *Plant Physiol.* **177**, 1639–1649 (2018).
47. M. Jokel, V. Nagy, S. Z. Tóth, S. Kosourov, Y. Allahverdiyeva, Elimination of the flavodiiron electron sink facilitates long-term H_2 photoproduction in green algae. *Biotechnol. Biofuels* **12**, 280 (2019).
48. S. Kosourov, M. Jokel, E. M. Aro, Y. Allahverdiyeva, A new approach for sustained and efficient H2 photoproduction by *Chlamydomonas reinhardtii*. *Energy Environ. Sci.* **11**, 1431–1436 (2018).
49. Y. Milrad, S. Schweitzer, Y. Feldman, I. Yacoby, Green algal hydrogenase activity is outcompeted by carbon fixation before inactivation by oxygen takes place. *Plant Physiol.* **177**, 918–926 (2018).
50. V. Nagy *et al*., Water-splitting-based, sustainable and efficient H_2 production in green algae as achieved by substrate limitation of the Calvin-Benson-Bassham cycle. *Biotechnol. Biofuels* **11**, 69 (2018).
51. A. Santana-Sanchez *et al*., Flavodiiron proteins 1-to-4 function in versatile combinations in O_2 photoreduction in cyanobacteria. *eLife* **8**, e45766 (2019).
52. P. J. Graham, B. Nguyen, T. Burdyny, D. Sinton, A penalty on photosynthetic growth in fluctuating light. *Sci. Rep.* **7**, 12513 (2017).
53. S. B. Mellor *et al*., Defining optimal electron transfer partners for light-driven cytochrome P450 reactions. *Metab. Eng.* **55**, 33–43 (2019).
54. L. M. Lassen *et al*., Anchoring a plant cytochrome P450 via PsaM to the thylakoids in *Synechococcus* sp. PCC 7002: Evidence for light-driven biosynthesis. *PLoS One* **9**, e102184 (2014).
55. S. B. Mellor *et al*., Fusion of ferredoxin and cytochrome P450 enables direct light-driven biosynthesis. *ACS Chem. Biol.* **11**, 1862–1869 (2016).
56. A. Kanygin *et al*., Rewiring photosynthesis: A photosystem I-hydrogenase chimera that makes H_2 in vivo. *Energy Environ. Sci.* **13**, 2903–2914 (2020).
57. J. Appel, V. Hueren, M. Boehm, K. Gutekunst, Cyanobacterial in vivo solar hydrogen production using a photosystem I–hydrogenase (PsaD-HoxYH) fusion complex. *Nat. Energy* **5**, 458–467 (2020).
58. M. Ihara *et al*., Light-driven hydrogen production by a hybrid complex of a [NiFe]-hydrogenase and the cyanobacterial photosystem I. *Photochem. Photobiol.* **82**, 676–682 (2006).
59. I. Yacoby *et al*., Photosynthetic electron partitioning between [FeFe]-hydrogenase and ferredoxin:$NADP^+$-oxidoreductase (FNR) enzymes in vitro. *Proc. Natl. Acad. Sci. U.S.A.* **108**, 9396–9401 (2011).
60. D. Kannchen *et al*., Remodeling of photosynthetic electron transport in Synechocystis sp. PCC 6803 for future hydrogen production from water. *Biochim. Biophys. Acta Bioenerg.* **1861**, 148208 (2020).
61. D. Leister, Experimental evolution in photoautotrophic microorganisms as a means of enhancing chloroplast functions. *Essays Biochem.* **62**, 77–84 (2018).
62. D. Leister, Genetic engineering, synthetic biology and the light reactions of photosynthesis. *Plant Physiol.* **179**, 778–793 (2019).
63. H. Kirst, C. Formighieri, A. Melis, Maximizing photosynthetic efficiency and culture productivity in cyanobacteria upon minimizing the phycobilisome light-harvesting antenna size. *Biochim. Biophys. Acta* **1837**, 1653–1664 (2014).
64. J. H. Kwon, G. Bernát, H. Wagner, M. Rögner, S. Rexroth, Reduced light-harvesting antenna: Consequences on cyanobacterial metabolism and photosynthetic productivity. *Algal Res.* **2**, 188–195 (2013).
65. M. A. Ware, D. Hunstiger, M. Cantrell, G. Peers, A chlorophyte alga utilizes alternative electron transport for primary photoprotection. *Plant Physiol.* **183**, 1735–1748 (2020).
66. A. R. Grossman, K. R. M. Mackey, S. Bailey, A perspective on photosynthesis in the oligotrophic oceans: Hypotheses concerning alternate routes of electron flow. *J. Phycol.* **46**, 629–634 (2010).
67. M. S. Roth, D. J. Westcott, M. Iwai, K. K. Niyogi, Hexokinase is necessary for glucose-mediated photosynthesis repression and lipid accumulation in a green alga. *Commun. Biol.* **2**, 347 (2019).
68. A. Cordara *et al*., Analysis of the light intensity dependence of the growth of *Synechocystis* and of the light distribution in a photobioreactor energized by 635 nm light. *PeerJ* **6**, e5256 (2018).
69. C. C. Hall *et al*., "Photosynthetic measurements with the Idea Spec: An integrated diode emitter array spectrophotometer/fluorometer" in *Photosynthesis Research for Food, Fuel and the Future*, T. Kuang, C. Lu, L. Zhang, Eds. (Springer, Berlin, Heidelberg, 2013), pp. 184–188.
70. P. J. Ralph, R. Gademann, Rapid light curves: A powerful tool to assess photosynthetic activity. *Aquat. Bot.* **82**, 222–237 (2005).
71. N. R. Baker, J. Harbinson, D. M. Kramer, Determining the limitations and regulation of photosynthetic energy transduction in leaves. *Plant Cell Environ.* **30**, 1107–1125 (2007).